C. R. Mecanique 338 (2010) 604–614

Contents lists available at ScienceDirect

Comptes Rendus Mecanique

www.sciencedirect.com

Micromechanics of granular materials

Discrete numerical investigation of the ratcheting phenomenon in granular materials

Analyse numérique discrète du phénomène de cliquet dans les matériaux granulaires

Francesco Calvetti *, Claudio di Prisco

Dipartimento di Ingegneria Strutturale, Politecnico di Milano, Piazza Leonardo da Vinci, 32, 20133 Milano, Italy

ARTICLE INFO

Article history:
Available online 25 October 2010

Keywords:
Granular materials
Incremental behaviour
Distinct elements
Cyclic loading
Ratcheting

Mots-clés :
Matériaux granulaires
Comportement incrémentale
Éléments discrets
Chargement cyclique
Cliquet

ABSTRACT

Several relevant geotechnical works, such as railway and road embankments, offshore foundations and vibrating machine foundations, are affected by the progressive accumulation of irreversible settlements. These latter represent the macroscopic evidence of the progressive rearrangement of particles under cycling loading, which is commonly referred to, in the literature, as ratcheting. This phenomenon is well known, but it is quite difficult to describe it by means of an appropriate constitutive model. As a consequence, the evaluation of durability of the aforementioned structures remains an open problem. In this article, the phenomenon will be approached by employing a Distinct Element model capable of describing the evolution of the microstructure induced by cyclic mechanical perturbations. Several analyses are performed in order to stress the influence of both the stress level and loading history on the mechanical response of a numerical model of a sand specimen. The numerical analyses are intended to provide an experimental background for conceiving a simplified macro approach based on generalised plasticity theory. In particular by means of probe test the plastic potential and the hardening parameters will be defined as a function of the current stress state and loading history.

RÉSUMÉ

Plusieurs travaux géotechniques, tels que les remblais des chemins de fer et des routes, les fondations *offshore* et celles des machines vibrantes, sont affectées par l'accumulation progressive des déformations irréversibles. Cela représente la réorganisation progressive des particules sous chargement cyclique, ce qui est communément appelé dans la littérature comme effet de cliquet. Ce phénomène est bien connu mais tout difficile à quantifier a travers d'un modèle constitutif approprié. Dans cet article, ce phénomène sera abordé en employant la méthode des éléments discrets pour décrire l'évolution de la structure induite par les perturbations cycliques mécaniques. Plusieurs essais numériques sont effectués afin d'évaluer l'influence du niveau de chargement et de la densité relative sur la réponse mécanique. Les analyses numériques sont destinées à fournir une base expérimentale pour concevoir une approche simplifiée basée sur la plasticité généralisée. En particulier par des sondages incrémentaux l'évolution du potentiel plastique et des paramètres d'écrouissage seront étudiés.

* Corresponding author.
E-mail addresses: francesco.calvetti@polimi.it (F. Calvetti), claudio.diprisco@polimi.it (C. di Prisco).

1631-0721/$ – see front matter
doi:10.1016/j.crme.2010.09.006

1. Introduction

The incremental behaviour of granular materials is the subject of many articles available in the literature, which is justified by the fact that the modelling of such materials has to account for relevant features such as non-linearity, irreversibility (or incremental non-linearity), stress dependency, not to mention the phenomena that characterise cyclic loading, such as the progressive accumulation of irreversible strains. The typical testing program for studying the incremental behaviour consists in the so called "stress-probing experiments", i.e., in applying a series of stress increments to a number of identical specimens, and measuring the corresponding incremental strains. Typically, the stress increments (probes) have identical magnitude, but point in different directions of the stress space; unloading to the initial stress state is often included in the testing program, i.e., one (single) loading–unloading cycle is performed. Variations of such programs are represented by cyclic tests, where the stress increment is repeatedly applied and then removed.

This type of testing may be performed both in the laboratory and numerically by using discrete tools, either in the domain of "Contact dynamics" or "Molecular dynamics" (also called "Distinct Element Method" or DEM). Actually, carrying out laboratory experiments of this kind [1] is extremely difficult: in fact, as many separate tests are needed as the number of stress probes, with the additional requirement that in all tests an identical sand specimen has to be fabricated and brought to exactly the same state. Moreover, the distinction between reversible and irreversible components of the total measured strain increment is impossible in the laboratory, unless loading–unloading cycles are performed, and the unloading phase is assumed to be elastic (which is only as a first approximation of reality, as numerically shown in [2]). The first DEM investigation of the incremental behaviour of granular materials was performed by using a 2D model made of an assembly of disks [3,4]. For such an idealised and 2D material, the obtained incremental response was satisfactorily interpreted in terms of a classical plasticity theories (i.e., elasto-plasticity with single mechanism), provided that a non-associated flow rule was adopted.

More recently, simulations have been performed using a 3D DEM model that was previously calibrated to match quantitatively the mechanical behaviour of Hostun sand [2]. These simulations included testing of virgin and overconsolidated specimens, under both axisymmetric and deviatoric stress probing. The results obtained in axisymmetric conditions for normally consolidated specimens, confirmed the previously mentioned findings, in particular the existence of yield surface, f, and plastic potential, g. On the contrary, for over-consolidated specimens or under more complex loading conditions, the classical elasto-plastic model is found to be inadequate (in particular it is no longer possible to define the functions f and g), and more complex constitutive models, such as generalised plasticity [5], are necessary to describe the observed behaviour [6]. The microscopic mechanisms that determine the macroscopically observed behaviour are studied in [7] and [8], where a correlation is shown between the magnitude and direction of irreversible strains and the occurrence of particle slip.

Another important limitation of classical elasto-plastic models is that they are not capable of describing the cyclic behaviour of granular materials. In fact, a progressive accumulation of strains is observed to occur experimentally, even for low amplitude cycles (i.e., cycles that would lie inside the yield surface, as defined in classical plasticity). Possibly, the most relevant example of such behaviour is represented by liquefaction of loose sand under cyclic loading [9], which may affect the stability of foundations during earthquakes.

The accumulation of permanent strain per cycle, when granular materials are subjected to loading–unloading stress cycles with amplitudes well below the yield limit was shown in [10], on the basis of numerical experiments performed on a two-dimensional model of polygonal particles. Similar numerical tests, performed on assemblies of disks, show that the permanent strain accumulation becomes independent of the number of cycles after a short transient regime [11]. From a micromechanical point of view, the observed macroscopic strains are associated to the evolution of the contact network, which in turn is due to relative sliding of particles at contacts [12].

Starting from the results available in the reported literature, the aim of this article is to study the cyclic behaviour of granular materials, by testing a 3D numerical model. With respect to previous analyses, the main features of this model are that it is made of an assembly of spheres, whose macroscopic behaviour was preliminary calibrated to match the behaviour of a real sand (namely Ticino river sand), as it will be recalled in the following. In particular, through the numerical tests presented in this paper, the influence of relative density and stress level on the accumulation of permanent strains are studied.

2. Numerical analyses

The simulations described in this article are performed using the code PFC3D that models assemblies of spheres. PFC3D implements the classical Distinct Element Method [13], where particles are rigid but contacts are considered deformable, i.e., particles may overlap at contacts, and contact forces are evaluated accordingly. In particular, in PFC3D normal contact forces are computed as: $F_N = k_N \cdot U_N$, where k_N is the normal stiffness of the contact and U_N is current particle overlap. On the contrary, tangential forces are computed incrementally (over each time-step): $\Delta F_S = k_S \cdot \Delta U_S$, where k_S is the shear stiffness of the contact and ΔU_S is the incremental tangential displacement. Local slip is introduced by limiting the current value of tangential contact forces: $F_S \leqslant F_N \cdot \tan(\Phi_\mu)$, where Φ_μ represents the interparticle friction angle. As usual in DEM approaches, both the equation of motion (for each particle) and the non-linear contact constitutive equations (at each

Table 1
Benchmark tests.

Test #	*DR* (%)	p' (kPA)	Type
1	47	110	calibration
2	46	200	prediction
3	41	300	prediction
4	72	100	prediction
5	74	200	prediction
6	75	300	prediction

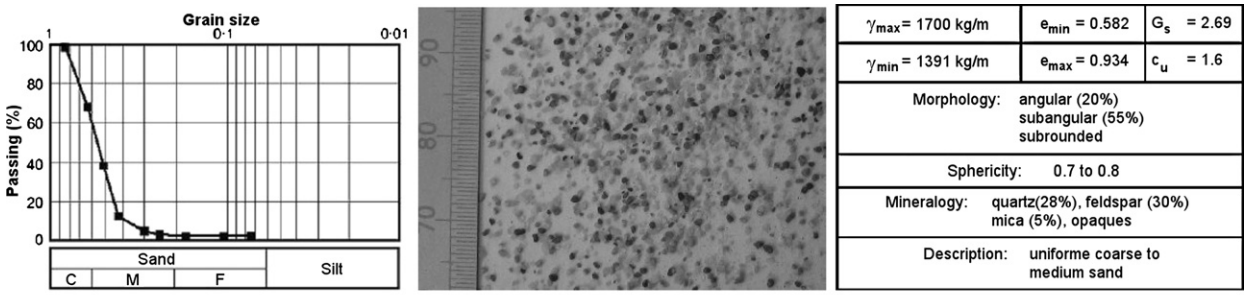

(a) grain-size curve (b) closeup grain picture (c) data-sheet

Fig. 1. Description of Ticino river sand, after [15].

contact) are integrated in time by means of an explicit finite difference scheme. Numerical, non-viscous, damping can be introduced in order to increase energy dissipation in addition to that produced by the interparticle sliding mechanism.

2.1. Description of the numerical model

For the simulations presented in this article, the numerical model introduced during the GEODIS project is employed [14]. GEODIS is a benchmark devoted to the assessment of predictive capabilities of discrete numerical models, and it takes as reference the results of a series of triaxial (axisymmetric) compression tests performed on Ticino river sand [15], as shown in Table 1.

The chosen modelling approach is based on the reproduction of the key factors that determine the mechanical behaviour of sand, i.e., grain size curve (Fig. 1(a)), porosity or relative density (Table 1), and particle shape (Figs. 1(b) and 1(c)). Grain size curve and porosity of the numerical model were taken directly from the given data, with relative density values rounded to $DR = 45\%$ and 75%. The differences between the spherical shape of model particles and the actual shape of Ticino sand grains, were taken into account by inhibiting particle rotations and calibrating the interparticle friction to match the results of the calibration test (test #1 of Table 1). In fact, assemblies of circular particles are characterised by unrealistically large particle rotations, which yields to very low friction angles, $\Phi < 30°$, irrespective of the interparticle friction angle, as experimentally [16] and numerically observed [17,18].

A very low value of numerical damping, δ, was used during the GEODIS benchmark simulations ($\delta = 5\%$). This value is to be compared to the default PFC3D value for static analysis, which is as large as $\delta = 70\%$: in fact, the use of large damping values is misleading, in that it may yield to apply larger loading rates than allowed in quasi-static conditions. The choice of $\delta = 5\%$ is maintained for the simulations presented in this paper. Full details regarding the adopted modelling approach and the discussion about its advantages and limitations are given in [14].

In order to limit the number of particles to about 5000, which provides a good compromise between model representativeness and saving of computational time, the PFC3D model (Fig. 2) reproduces a small cubic sample of the Ticino sand specimen, with side equal to 1.0 cm. The boundary is defined by six smooth plates (not shown in Fig. 2) normal to the X–Y–Z reference axes. Three plates (one for each axis) are fixed, the remaining three plates are used to apply loading conditions (directly setting their velocity, or adjusting it through a servo-control for stress controlled tests). All the simulations described in this paper are performed under the condition $\sigma_x = \sigma_y$. Thanks to the initial isotropy of the specimen, the measured strains are $\epsilon_x = \epsilon_y$ with negligible deviations. For this reason, although the specimen is cubic (which allows to apply more general loading conditions, as in [8] and [6]), the performed tests are in all respects equivalent to axisymmetric ones. The usual stress and strain invariants will be therefore defined and used to describe the tests: confining pressure, $p' = \frac{1}{3}(\sigma_z + 2\sigma_x)$; deviatoric stress, $q = \sigma_z - \sigma_x$; volumetric strain, $v = \epsilon_z + 2\epsilon_x$; deviatoric strain, $e = \frac{2}{3}(\epsilon_z - \epsilon_x)$.

The adopted set of parameters for the Ticino sand model is reported in Table 2; the corresponding sets of calibrated parameters for Hostun sand [2] and Adige river sand [19], are reported too for comparison. As discussed in [14], when round particles are employed the effects of individual grain properties (shape and mineralogy) can be reproduced only by an appropriate choice of micromechanical parameters and in particular, as to shape is concerned, interparticle friction is the

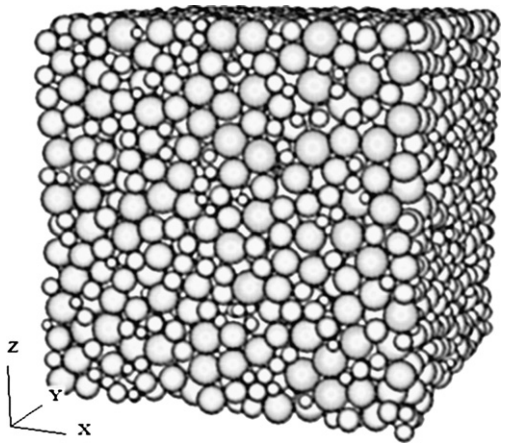

Fig. 2. DEM model of a Ticino sand specimen, after [14].

Table 2
DEM parameters calibrated for different types of sand.

Sand type	Φ_μ	k_N/D	k_S/k_N	Reference
Ticino river	18.0°	420 MPa	0.25	this paper and [14]
Hostun	19.3°	330 MPa	0.25	[2]
Adige river	17.5°	250 MPa	0.25	[19]

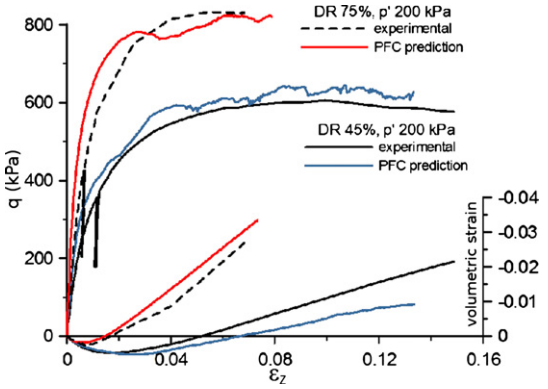

Fig. 3. DEM model predictions, after [14].

key parameter. It is worth noting that the Φ_μ values reported in Table 2 are smaller than the surface friction angle, which means that the rotation constraint over-corrects the effects of the spherical shape of numerical elements.

The predictions of the model, in terms of stress–strain and volumetric curves, are shown in Fig. 3 with reference to two specimens ($DR = 45\%$ and 75%) tested at $p' = 200$ kPa. It is worth noting that these results refer to tests performed at different confining pressures and different relative density (in the second case) than those of the test used for calibration (test #1, Table 1). These conditions represent a very demanding benchmark for the model, whose performance and reliability appear to be highly satisfactory. A complete description and discussion of the results are given in [14].

2.2. Plan of the simulations

As previously reported, the simulations that will be presented in this article are performed with the aim of highlighting the effects of stress level and relative density on the accumulated irreversible strains. For this reason, the two specimens with 45% and 75% of relative density are tested, and a preliminary vertical compression with $p' = 200$ kPa is performed on both of them (same tests as in Fig. 3). During the preliminary compression several stress states are recorded (Fig. 4); then, starting form these stress states, a series of loading–unloading cycles is performed. With reference to the data of Table 3, both the actual deviatoric stress, q, and the mobilised resistance, η, are considered for the following interpretation of the results, in particular as far as the comparison between the behaviour recorded at $DR = 45\%$ and 75%. For each specimen, mobilised resistance is defined as the ratio between the current deviatoric stress, q, and its peak $q_{\max}\%$ (see Fig. 4). Note that, for instance, states B and G have the same q, but very different η, as expected, because of their different intrinsic

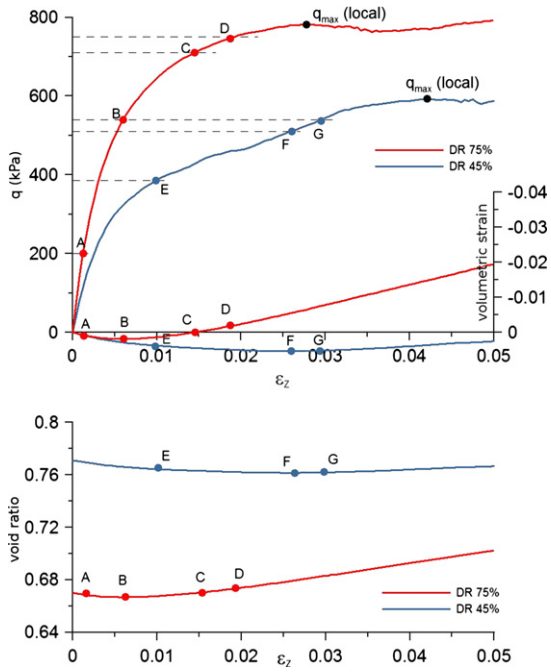

Fig. 4. Preliminary compression and initial stress states for cyclic testing.

Table 3
Investigated stress states.

Point	*DR* %	q kPa	$\eta = q/q_{\max}$ %
A	75	200	26
B	75	540	69
C	75	710	90
D	75	755	97
E	45	385	66
F	45	510	87
G	45	540	92

peak resistance (which, in turn, is a function of their initial *DR*, or initial porosity); on the other side, states *B* and *E* share virtually the same $q/q_{\max}$ ratio despite different values of q and porosity. The same applies to states *C*, *F* and *G*.

During cycling, the loading direction is the same as that of previous compression, i.e., cycles are characterised by $\Delta\sigma_x = \Delta\sigma_y = 0$. Therefore, the norm of the stress increment is coincident with that of $\Delta\sigma_z$, which in turn is set to 10 kPa, the same value adopted during previous studies [2,7,8].

The applied stress increments and a typical response (state *B* of Table 3) are illustrated in Fig. 5, for a preliminary qualitative discussion.

The stress rate adopted is determined as a compromise between two opposite requirements: in fact, the specimen has to be tested in quasi-static and rate-independent conditions, but stress rate should be as high as possible in order to reduce computation time. Under this constraint, it is worth noting that generally the first cycle was diluted over a larger number of calculation steps, as shown in Fig. 5(a). As an additional precautionary measure, at the end of each stress increment the stress is kept constant for a certain number of cycles, until strain rate becomes exactly zero. As to the chosen stress rate, it is well known that irreversible strains correspond to particle slip and fabric rearrangement [7,8] which take time to fully develop; on the contrary, the elastic response is immediate in quasi-static conditions [20]. In fact, the irreversible strains recorded upon the first cycle, ϵ^{p1}, are much larger than those associated to a generic cycle n, ϵ^{pRn}, as shown in Fig. 5(b). However, despite individually ϵ^{pRn} tend to decrease with n, their accumulation yields to a clearly non-negligible "ratcheting strain", ϵ^{pR}. This behaviour will be studied quantitatively in Section 3.

It is interesting to note that the analysis of a typical stress–strain curve (Fig. 6) reveals that the unloading–reloading phases are essentially reversible, with the exception of the very last part of the reloading phase (see also Figs. 8 and 7 for further evidence); this demonstrates that plastic deformations start to occur in the close vicinity of what classical plasticity would define "yield surface".

Finally, some minor features of the stress–strain curve need further discussion: (a) the initial stiffness of the first loading phase is virtually coincident with that of the unloading/reloading cycles, which means that the very initial response is elastic; (b) at the end of the first loading step, a small accumulation of strains is observed under constant stress. Although

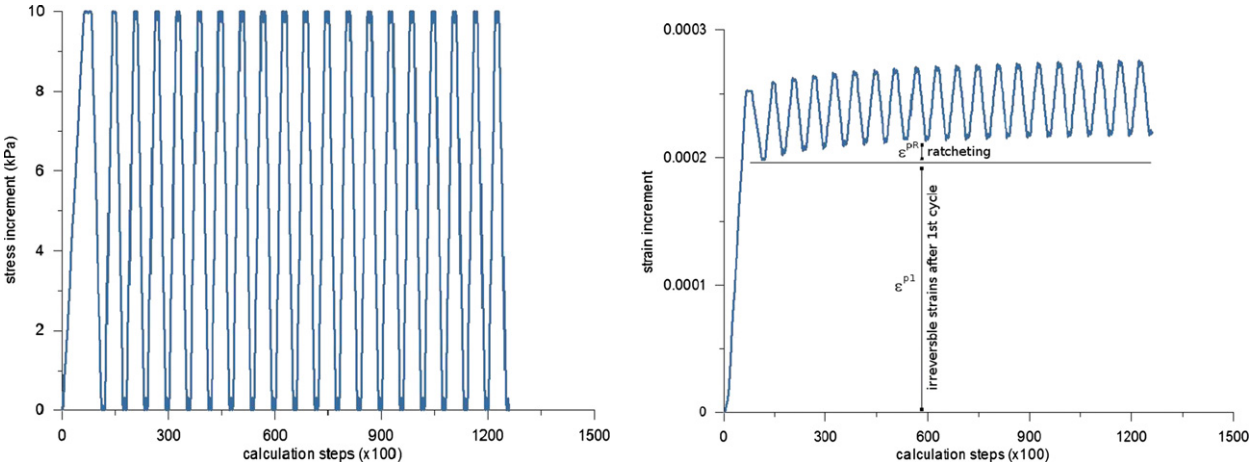

(a) stress increments (b) strain response

Fig. 5. Cyclic loading programme, initial state *B* taken as reference.

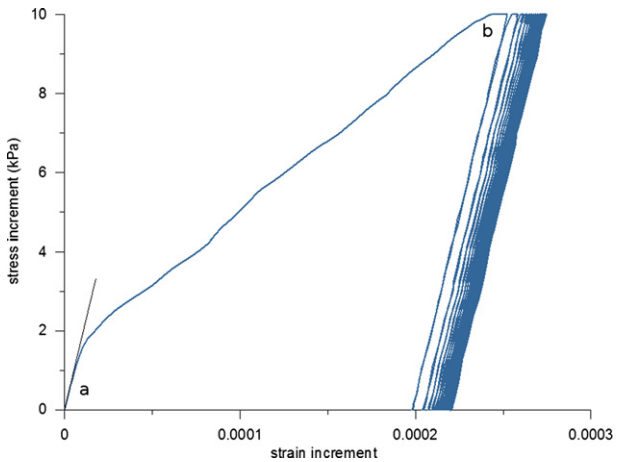

Fig. 6. Stress–strain curve, initial state *B* taken as reference.

both these issues could be completely solved by applying a slower stress-rate, it is worth noting that irreversible strains are dominant during the first cycle, but they tend to progressively decrease in the following ones. For this reason, the previously described issues are considered completely irrelevant as to the interests of this paper, which is focused on the accumulation of strains with cycling.

3. Numerical results

In this section results will be progressively introduced by considering several different aspects of the incremental behaviour, starting from the qualitative analysis of the results and the evaluation of the plastic potential evolution. Finally the analysis of the magnitude of accumulated irreversible strains is presented.

In Fig. 7 the progressive accumulation of irreversible strains over cycling is shown. As to the denser specimen (*DR* 75%), the influence of initial mobilised resistance is clearly visible by comparing the behaviour corresponding to initial states *A*, *B*, *C* and *D*. As expected, for the same initial deviator (initial points *B* and *G*) the specimen with *DR* 45% is characterised by much larger deformations. However, it is more interesting to observe, from a qualitative point of view, that for large values of mobilised resistance, η, the response of the less dense specimen becomes much more irregular than that of the denser one. In particular, despite a larger value of η the test starting at point *G* is characterised by first cycle irreversible strains, ϵ^{p1}, smaller than those recorded starting at point *F*. Then its response shows a sharp increase of irreversible strains during cycle #4, while the behaviour recorded during following cycles is more regular. Further comments about this evidence, which is obviously associated to the metastable fabric of the specimen, will be presented in the following.

Fig. 8 reports the complete set of strain increments as recorded during the cyclic tests. Again, the large dependency of the strain response for the denser material is evident. The progressive evolution of the direction of accumulated strains with the initial stress level is also clearly shown, which is associated to the progressive rotation of the plastic potential

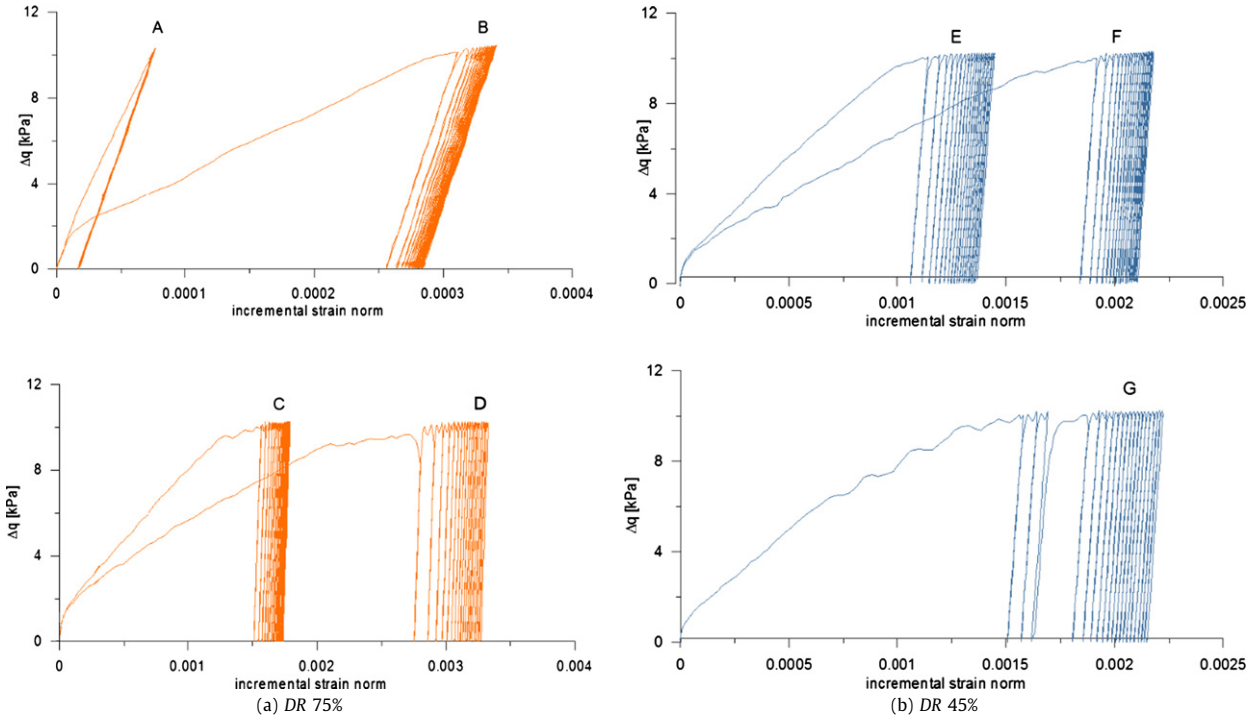

Fig. 7. Norm of plastic strains as a function of number of cycles.

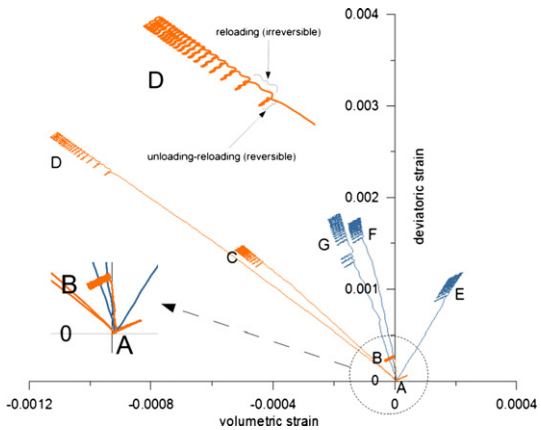

Fig. 8. Strain response, all investigated points.

(see Fig. 9). It is worth to note that, on the contrary, the direction of strains associated with the unloading parts of the cycles are almost independent on relative density and initial stress level. Since strains during unloading can be, as a first approximation, considered reversible (as previously discussed), this evidence is of great help in detecting the triggering of irreversible strains during the reloading parts of the cycles. In fact, the results of Fig. 8 confirm the previous consideration that irreversible strains are accumulated only during the very last part of the reloading phase, which is here characterised by a sharp change in the incremental strain direction.

In Fig. 9(a) the irreversible strains corresponding to the end of each cycle are shown, for all the performed tests. As a first approximation, for given initial state and relative density, as strains are progressively accumulated their direction remains constant. This result might be interpreted by adopting the concept of plastic potential. However, a more refined analysis highlights a peculiar distinction between the denser and the looser specimen (Fig. 9(b)). In fact, for *DR* 45% only, the direction of incremental irreversible strains as determined during the first cycle, is slightly different from that corresponding to the following ones, where ratcheting strains are accumulated. This rotation highlights an increase of the compactant tendency typical of initial state *E*, and a reduction of dilatancy at initial states *F* and *G*. In addition to this general trend, a more accurate analysis of the behaviour recorded at point *G* reveals an irregular variation of the direction of incremental

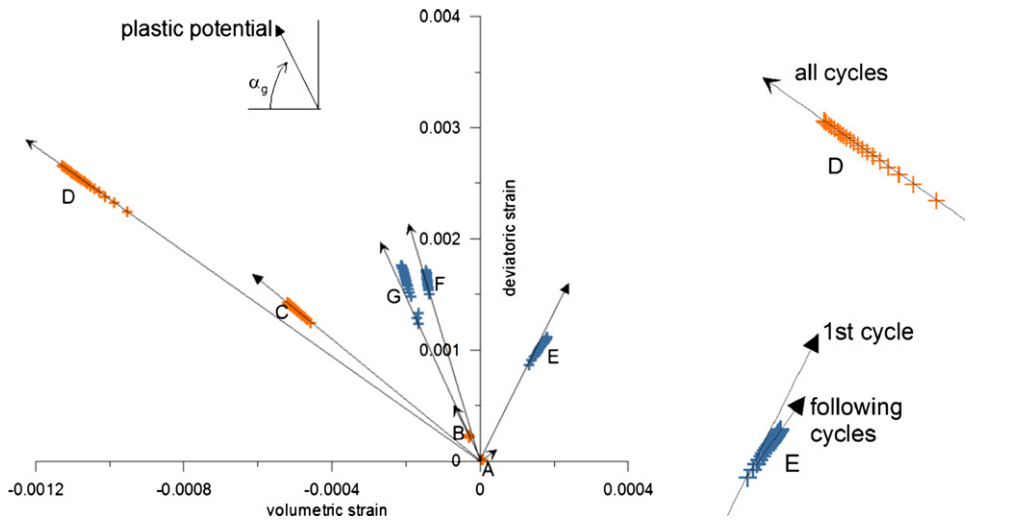

(a) overview (b) typical response for *DR* 75% and 45%

Fig. 9. Cyclic response, irreversible strains.

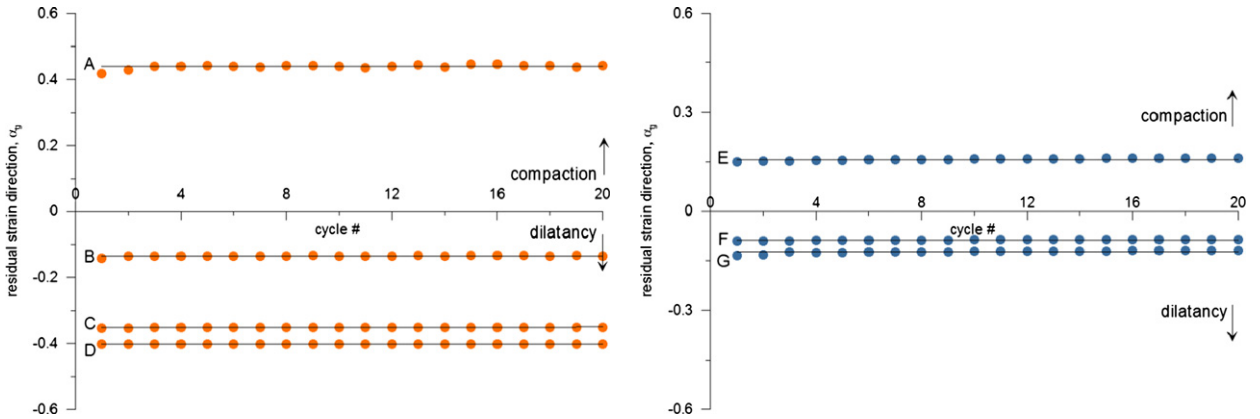

(a) *DR* 75% (b) *DR* 45%

Fig. 10. Direction of plastic potential.

residual strains, especially during the first 4 cycles, in analogy to what observed as to the norm of irreversible strains (Fig. 7(b)).

The progressive rotation of the plastic potential is also visible in Fig. 10, where the direction α_g, as defined in Fig. 9(a), is plotted. From these data, it is clear that the increase of η corresponds to a progressive increase of dilatancy, for both relative densities. The variation is much more pronounced for the denser specimen, while the looser one exhibits minor variations. This result is in agreement with the fact that the porosity of the specimen with *DR* 45% remains almost unchanged during the preliminary compression (see Fig. 4). Compared to the influence of the initial state of stress, the observed slight rotation of the plastic potential after the first cycle, and the irregular trend recorded at point *G*, are negligible in Fig. 10.

In order to interpret the irregular behaviour observed at *DR* 45%, it may be useful to consider the evolution of the specimen fabric. This latter can be globally studied by considering the evolution of porosity and mean contact forces (Fig. 11), and the variation of the overall number of contacts (Table 4).

As a first comment, for all the investigated initial states, the mean value of the normal contact forces tends to increase. This compensates the decrease of the number of contacts, as expected considering that after each cycle the same state of stress is recovered. As a general trend, porosity tends to decrease with cycling at point *E*, remains almost constant at point *F*, and tends to increase at point *G*, in agreement with previously commented results. However, it is worth observing that the evolution of porosity at point *G* is very irregular, in particular during the first cycles where a temporary inversion of the general trend is observed. In fact, during cycle #3, porosity decreases but at the same time the mean contact force increases, which indicates a sensible loss of contacts. These unique (with reference to the whole set of performed simulations) conditions are those that favour the observed large increase of irreversible strains during the following cycle #4 (see Fig. 7 and previous comments).

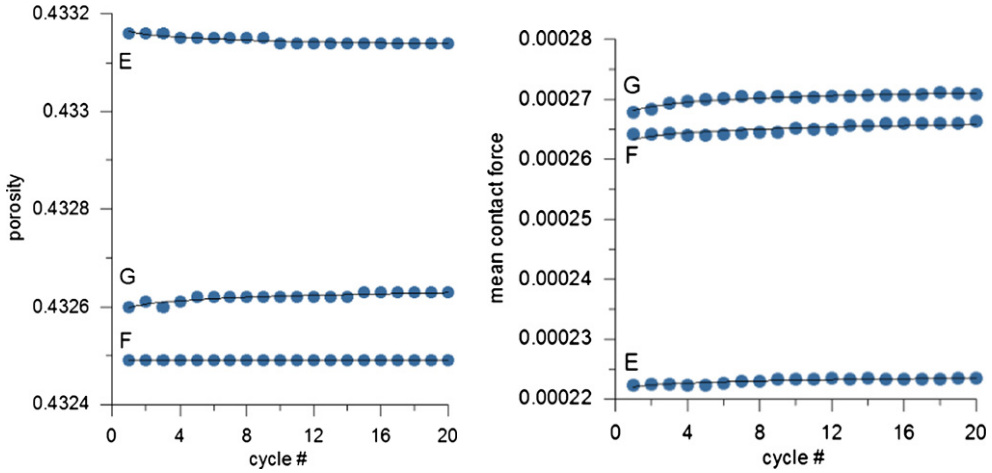

(a) porosity (b) mean value of normal contact forces

Fig. 11. Evolution of porosity and mean contact forces (*DR* 45%).

Table 4
Number of contacts, n_c.

Point	n_c, initial	n_c, after cycle #20
E	6631	6553
F	6480	6382
G	6439	6331

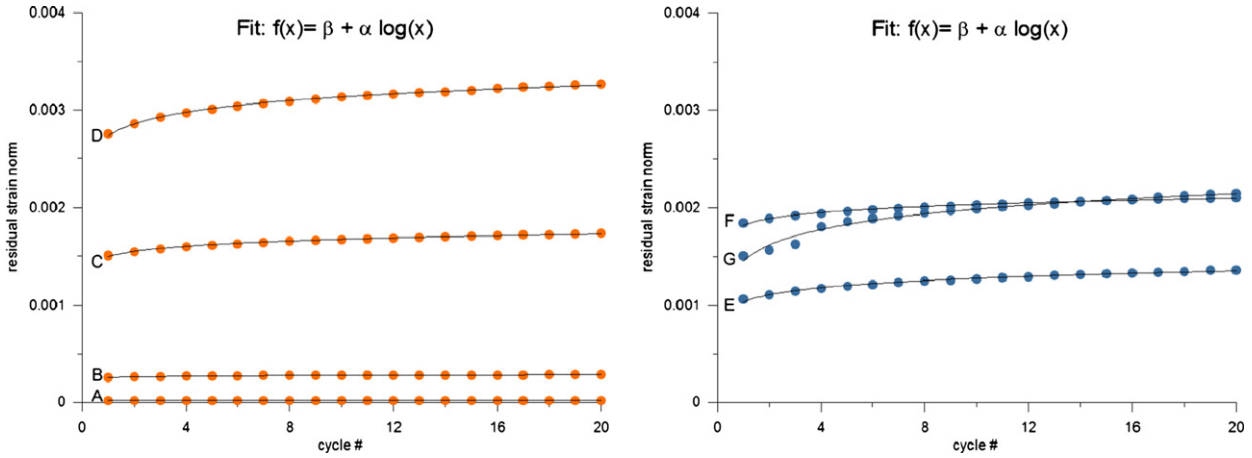

(a) *DR* 75% (b) *DR* 45%

Fig. 12. Norm of irreversible strains.

3.1. Quantitative analysis of the accumulation of irreversible strains

The evolution of the norm of irreversible strains with cycling is shown in Fig. 12. As a first approximation, if the previously discussed irregularities are neglected, the numerical results may be very effectively interpolated by introducing the following function: $\epsilon^p(n) = \beta + \alpha \log(n)$, where n is the number of cycles. β and α are two parameters that depend on relative density and initial stress state (see Fig. 13). In particular, β represents the irreversible strain after the first cycle, i.e., it corresponds to ϵ^{p1} of Fig. 5(b); in turn, α describes the rate of accumulation of irreversible strains, i.e., it determines ϵ^{pR}.

In Fig. 13 α and β are plotted versus the deviator stress, q, and the mobilised strength, η, for all the investigated stress states. From a qualitative point of view, as expected, both α and β increase with q, in a very similar way; moreover, for the same q, both parameters are significantly smaller for the denser specimen. However, in order to highlight the effect of relative density, it is much more interesting to discuss the evolution of α and β with η. First of all, quantitatively, the logarithm of α and β is found to increase linearly with η. In addition, it is evident that the difference between the results obtained for the two specimens are very large for low mobilised strength, but they tend to vanish when the initial stress approaches failure. This results confirm, as expected, that the looser specimen is intrinsically more prone to undergo

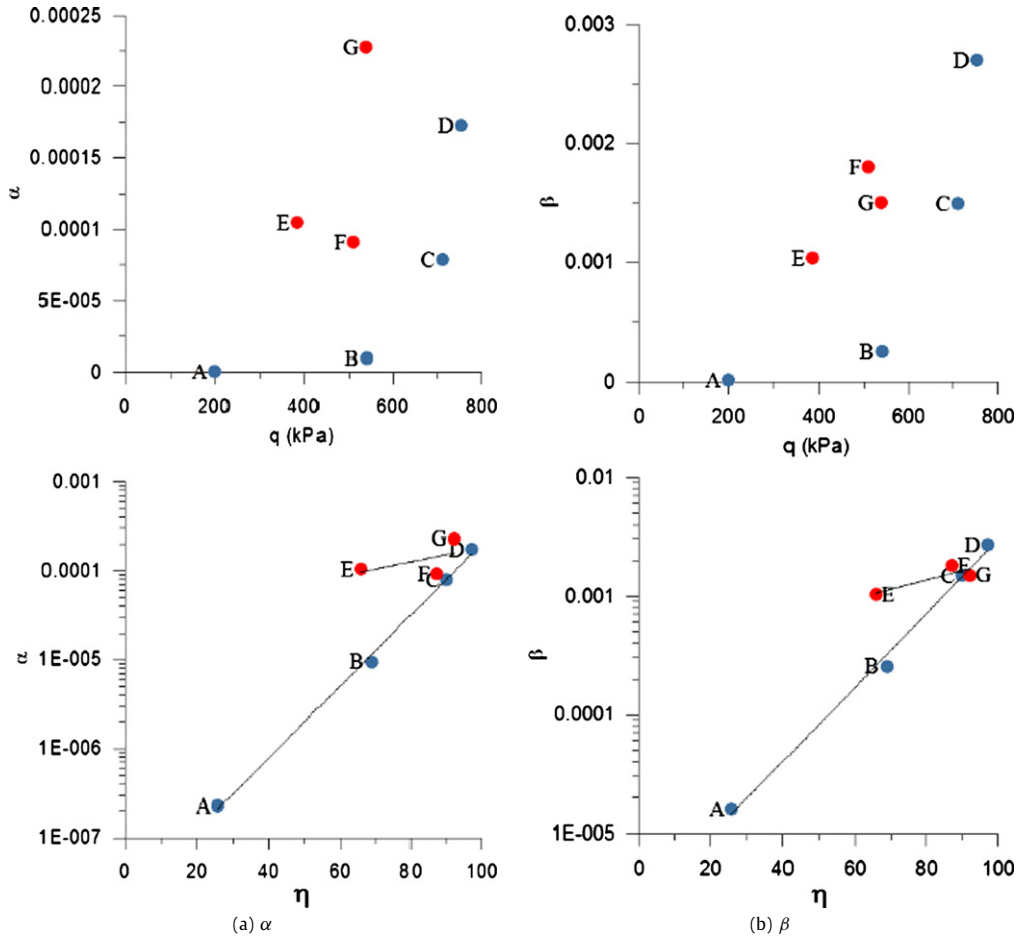

(a) α (b) β

Fig. 13. α and β as a function of stress level.

irreversible strains, but that as failure approaches the initial advantage of the denser specimen is progressively lost: this seems reasonable, if we consider that both specimens tend to a common critical state (which is not yet attained, for the considered stress states, see Fig. 4).

4. Conclusions and perspectives

In this article, a series of simulations have been performed to highlight the cyclic behaviour of a numerical model of Ticino sand.

The accumulation of plastic strains over cycling is observed to be depending on stress level and relative density, and some qualitative differences were observed as a function of relative density.

As a first approximation, the direction of plastic strains as determined during the first loading–unloading cycle remains constant during the following loops. The norm of accumulated strains is found to increase logarithmically with the number of cycles, without reaching a limit value. Further analyses, where a larger number of cycles is considered, are in due course, as well as other incremental loading directions are being currently investigated.

For the sake of simplicity, the results presented in this paper are referring to the macroscopically observed behaviour. Following the line of previous works, where irreversible deformations were correlated to particle slip, an analysis of the microscopic features will be presented in the future.

Acknowledgement

The support of Ce.A.S. and Itasca Consulting Group is gratefully acknowledged.

References

[1] P. Royis, T. Doanh, Theoretical analysis of strain response envelopes using incrementally non-linear constitutive equations, Int. J. Num. Anal. Meth. Geomech. 22 (1998) 97–132.

[2] F. Calvetti, G. Viggiani, C. Tamagnini, A numerical investigation of the incremental behaviour of granular soils, Rivista Italiana di Geotecnica 37 (3) (2003) 11–29.
[3] J.P. Bardet, J. Proubet, Application of micromechanics to incrementally nonlinear constitutive equations for granular media, in: J. Biarez, R. Gourvès (Eds.), Powders & Grains 1989, Balkema, Rotterdam, 1989, pp. 265–273.
[4] J.P. Bardet, Numerical simulations of the incremental responses of idealized granular materials, Int. J. Plast. 10 (8) (1991) 879–908.
[5] M. Pastor, O.C. Zienkiewicz, A.H.C. Chan, Generalized plasticity and the modelling of soil behaviour, Int. J. Num. Anal. Meth. Geomech. 14 (1990) 151–190.
[6] C. Tamagnini, F. Calvetti, G. Viggiani, An assessment of plasticity theories for modeling the incrementally nonlinear behaviour of granular soils, J. Engrg. Math. 52 (1–3) (2005) 265–291.
[7] F. Calvetti, Micromechanical inspection of constitutive modelling, in: C. Viggiani (Ed.), Constitutive Modelling and Analysis of Boundary Value Problems in Geotechnical Engineering, Hevelius, Benevento, 2003, pp. 187–216.
[8] F. Calvetti, C. Tamagnini, G. Viggiani, Micro-mechanics of the incremental response of virgin and preloaded granular soils to deviatoric stress probing, in: P.A. Vermeer, W. Ehlers, H.J. Herrmann, E. Ramm (Eds.), Continuous and Discontinuous Modelling of Cohesive-Frictional Materials, Taylor & Francis, 2004, pp. 121–133.
[9] G. Castro, Liquefaction and cyclic mobility of saturated sands, J. Geotech. Engrg., ASCE 101 (6) (1975) 551–569.
[10] F. Alonso-Marroquin, H.J. Herrmann, Ratcheting of granular materials, Phys. Rev. Lett. 92 (5) (2004) 543011–543014.
[11] R. Garcia-Rojo, F. Alonso-Marroquin, H.J. Herrmann, Characterization of the material response in granular ratcheting, Phys. Rev. E – Statist. Nonlinear Soft Matter Phys. 72 (4) (2005) 1–12.
[12] F. Alonso-Marroquín, H.B. Muhlhaus, H.J. Herrmann, Micromechanical investigation of granular ratcheting using a discrete model of polygonal particles, Particuology 6 (6) (2008) 390–403.
[13] P.A. Cundall, O.D.L. Strack, A discrete numerical model for granular assemblies, Géotechnique 29 (1) (1979) 47–65.
[14] F. Calvetti, Discrete modelling of granular materials and geotechnical problems, Eur. J. Environ. Civil Engrg. 12 (7–8) (1998) 951–965.
[15] G. Baldi, R. Bellotti, V. Ghionna, M. Jamiolkowski, E. Pasqualini, V. Crippa, P. Morabito, S. Pedroni, C. Fretti, D. Ostricati, Laboratory validation of in situ tests, in: AGI Golden Jubilee Volume for XI ICSMFE, 1985.
[16] A.E. Skinner, A note on the influence of interparticle friction on the shearing strength of a random assembly of spherical particles, Géotechnique 19 (1969) 150–157.
[17] A.S.J. Suiker, N.A. Fleck, Frictional collapse of granular assemblies, J. Appl. Mech., ASME 71 (2004) 350–358.
[18] F. Calvetti, R. Nova, Micromechanical approach to slope stability analysis, in: F. Darve, I. Vardoulakis (Eds.), Degradations and Instabilities in Geomaterials, Springer, 2004, pp. 235–254.
[19] F. Gabrieli, S. Cola, F. Calvetti, Use of an up-scaled dem model for analysing the behaviour of a shallow foundation on a model slope, Geomechanics and Geoengineering 4 (2) (2009) 109–122.
[20] F. Calvetti, Micromechanical investigation of the visco-plastic behaviour of granular materials, in: G.N. Pande, S. Pietrusczczak, N.F. Schweiger (Eds.) NUMOG, vol. VII, Balkema, Rotterdam, 1999, pp. 59–64.